Article

Chinese Science Bulletin

SPECIAL ISSUE: Molecular Materials and Devices
Progress of Projects Supported by NSFC

August 2013 Vol.58 No.22: 2753–2761
doi: 10.1007/s11434-013-5938-4

Design, synthesis and nonlinear optical properties of "dendronized hyperbranched polymers"

WU WenBo[1], HUANG LiJin[1], FU YingJie[1], YE Cheng[2], QIN JinGui[1] & LI Zhen[1*]

[1] *Department of Chemistry, Wuhan University, Wuhan 430072, China;*
[2] *Institute of Chemistry, Chinese Academy of Sciences, Beijing 100080, China*

Received January 31, 2013; accepted April 15, 2013

A new type of dendritic polymer, named dendronized hyperbranched polymer (DHP), was prepared successfully by the macromonomer approach. Thanks to the perfect 3D isolation effects, **DHPG1** exhibited good NLO property with d_{33} value of 133 pm/V, higher than its analogues of dendronized polymer and dendrimer, and its stability of NLO effect was also enhanced.

dendritic macromolecules, dendronized hyperbranched polymers, nonlinear optical

Citation: Wu W B, Huang L J, Fu Y J, et al. Design, synthesis and nonlinear optical properties of "dendronized hyperbranched polymers". Chin Sci Bull, 2013, 58: 2753–2761, doi: 10.1007/s11434-013-5938-4

The development of macromolecule fields was inseparable from synthetic polymers. The initial introduction of synthetic polymers in the 1830's is today reflected by an infinite number of structural variations that have ended in key components in products to meet the requirements of modern society [1]. For synthetic chemists, it is important to design and synthesize new types of functional polymers, to promote the development of the polymeric science. Dendritic macromolecules are a prime example of an important scientific breakthrough for the synthetic polymers from normal linear polymers [1]. Among them, dendrimers and hyperbrached polymers are the typical ones and already poised to make significant contributions to several areas of physical and biological science and engineering, due to their unique architectural and functional features [2–7]. Inspired by these encouraging results, by the attachment of the dendrimers to the linear polymeric backbone, chemistry researchers have designed a new architecture, termed as "dendronized polymers", since 1987 [8–10]. Following this idea, how about the introduction of the dendrimers to another dendritic polymeric system, for example, hyperbranched polymer (Figure 1)?

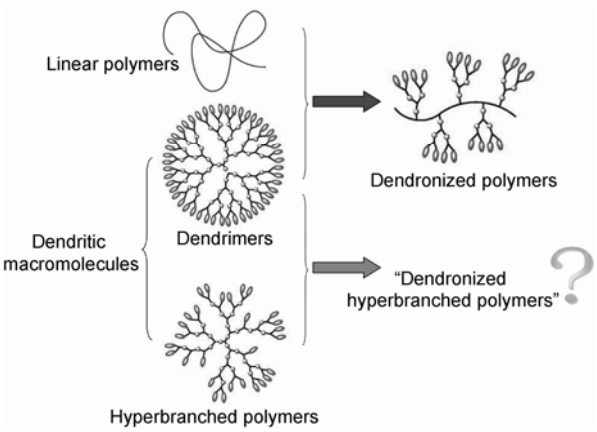

Figure 1 Schematic overview of different types of macromolecule and the premier idea in this communication.

In this article, we tried to introduce the low generation dendrimers into a hyperbranched polymeric backbone. Due to their architectural features, these new polymers were named as "dendronized hyperbranched polymers (DHP)" here. As we know, dendrimers are defect-free and perfect monodisperse, but the synthesis is usually tedious and difficult, while hyperbranched polymers are much easier to be

*Corresponding author (email: lizhen@whu.edu.cn; lichemlab@163.com)

obtained, but their structures are usually imperfect. In our opinion, DHP, with the new dendritic structure, should combine the advantages of dendrimers and hyperbranched polymers: the synthesis should be much easier than that of dendrimers, and their defect should be much less than those of hyperbranched polymers. Meanwhile, the topological structure of DHP should be much different from those of dendrimers and hyperbranched polymers. However, it is not clear what properties could be brought out by this topological structure. Furthermore, in this article, the introduced low generation dendriemrs consisting of nitro-based azobenzene chromophores, therefore, the final obtained DHPs could be applied to the second-order nonlinear optical field (NLO, one kind of materials with the promise of performance and cost improvements related to telecommunications, computing, embedded network sensing, THz wave generation and detection, and many other applications) [11]. Meanwhile, the three-dimensional (3D) spatial separation of the chromophore moieties endows the highly branched DHPs with favorable site isolation effect, which could minimize the strong intermolecular electrostatic interactions among chromophore moieties with high dipole moment, and thus enhance macroscopic optical nonlinearities, similar to dendrimers and hyperbranched polymers, according to site isolation principle [12–14] and the concept of "suitable isolation group" [15]. To our surprise, the obtained polymers demonstrated very good comprehensive performance: their NLO coefficient and stability were both improved, in comparison with their analogues of dendronized polymer and dendrimer. Herein, we would like to present the syntheses, characterization and properties of these new DHPs in detail.

1 Experimental

1.1 Materials and instrumentation

Tetrahydrofuran (THF) was dried over and distilled from K-Na alloy under an atmosphere of dry nitrogen. 3,6-Dibromo-9-(6-bromohexyl)-9H-carbazole (**S1**) and the NLO dendrons **G0-≡**, **G1-≡** and **G2-≡** were prepared in our previous work [16–19], and its synthetic route could be seen in scheme S1 in supporting information. Tris(4-(4,4,5,5-tetramethyl-1,3,2-dioxaborolan-2-yl)phenyl)amine (**S3**) was synthesized during normal procedure for the preparation of bronic ester by two steps, and its synthetic route was shown in Scheme S2. All other reagents were used as received.

^{1}H and ^{13}C NMR spectra were measured on a Varian Mercury300 or Varian Mercury 600 spectrometer using tetramethylsilane (TMS; δ = 0) as internal standard. The Fourier transform infrared (FTIR) spectra were recorded on a Perkin Elmer-2 spectrometer in the region of 3000–400 cm^{-1}. UV-Vis spectra were obtained using a Shimadzu UV-2550 spectrometer. Matrix-assisted laser desorption ionization time-of-flight mass spectra were measured on a Voyager-DE-STR MALDI-TOF mass spectrometer (MALDI-TOF MS; ABI, America) equipped with a 337 nm nitrogen laser and a 1.2 m linear flight path in positive ion mode. Elemental analyses (EA) were performed by a CARLOERBA-1106 micro-elemental analyzer. Gel permeation chromatography (GPC) was used to determine the relative molecular weights of polymers. GPC analysis was performed on a Waters HPLC system equipped with a 2690D separation module and a 2410 refractive index detector. Polystyrene standards were used as calibration standards for GPC. THF was used as an eluent, and the flow rate was 1.0 mL min^{-1}. Absolute molecular weights of the DHPs were measured by laser light scattering (LLS) technique (Down EOS). Thermal analysis was performed on NETZSCH STA449C thermal analyzer at a heating rate of 10°C min^{-1} in nitrogen at a flow rate of 50 cm^3 min^{-1} for thermogravimetric analysis (TGA). The thermal transitions of the polymers were investigated using a METTLER differential scanning calorimeter DSC822e under nitrogen at a scanning rate of 10°C min^{-1}. The thickness of the films was measured with an Ambios Technology XP-2 profilometer.

1.2 Synthesis

(1) Synthesis of compound **S2**. Compound **S1** (976 mg, 2.18 mmol) was dissolved in 12 mL DMF, and then sodium azide (260 mg, 4.0 mmol) was added. The mixture was stirred at 80°C over night. After being cooled, the solid salts were removed by filtration, and the filtrate was poured into water, then extracted with chloroform, and washed with brine and water for several times. The organic layer was dried over magnesium sulfate. The crude product was purified by column chromatography on silica gel using petroleum ether/chloroform (2/1, v/v) as eluent to afford white solid compound **S2** (898 mg, 99%). IR (KBr), υ (cm^{-1}): 2100 (–N_3). ^{1}H NMR ($CDCl_3$, 300 MHz) δ (TMS): 1.38 (s, br, 4H, –CH_2–), 1.52 (s, br, 2H, –CH_2–), 1.85 (m, 2H, –CH_2), 3.22 (t, J = 6.6 Hz, 2H, –CH_2N_3–), 4.26 (t, J = 6.6 Hz, 2H, –NCH_2–, 7.28 (d, 2H, ArH), 7.54 (d, J = 8.1 Hz, 2H, ArH), 8.15 (s, 2H, ArH). ^{13}C NMR ($CDCl_3$, 75 MHz) δ: 26.23, 26.49, 28.46, 29.58, 42.70, 50.99, 110.03, 111.65, 122.82, 128.65, 138.74. MALDI-TOF MS: calcd. for $C_{80}H_{77}N_{15}O_{14}$: m/z $[M+H]^+$ 450.17; found: m/z 449.94. $C_{18}H_{18}N_4Br_2$ (EA) (%) found: C, 48.67; H, 4.43; N, 12.01. Calcd. C, 48.02; H, 4.03; N, 12.45.

(2) Synthesis of monomer **MG0**. Chromophore **G0-≡** (124.1 mg, 2.0 mmol), compound **S2** (99.0 mg, 2.2 mmol), $CuSO_4{\cdot}5H_2O$ (10 mol%), $NaHCO_3$ (20 mol%), and ascorbic acid (20 mol%) were dissolved in THF (5 mL)/H_2O (1 mL) under nitrogen in a Schlenk flask. The mixture was stirred at room temperature for 3 h, then extracted with chloroform, and washed with brine. The organic layer was dried over anhydrous magnesium sulfate and purified by column chromatography using ethyl acetate/chloroform (1/2, v/v) as

eluent to afford red solid **MG0** (102 mg, 95%). IR (KBr), υ (cm^{-1}): 1723 (C=O), 1511, 1341 (–NO_2). ^{1}H NMR ($CDCl_3$, 300 MHz) δ (TMS): 1.26 (s, br, 4H, –CH_2–), 1.78 (m, 4 H, –CH_2–), 2.32 (t, J = 6.9 Hz, 2H, –CH_2C–), 2.99 (t, J =7.2 Hz, 2H, –CH_2–), 3.94 (t, J = 5.4 Hz, 2H, –NCH_2–), 4.21 (t, J = 6 Hz, 4H, –NCH_2–), 4.26 (t, J =6 Hz, 2H, –OCH_2–), 4.57 (t, J = 6 Hz, 4H, –$COOCH_2$–), 6.96 (d, J = 4.5 Hz, 2H, ArH), 7.24 (t, br, J = 5.7 Hz, 5H, ArH), 7.40–7.47 (m, 4H, ArH), 7.52–7.58 (m, 4H, ArH), 7.59 (d, J = 4.8 Hz, 2H, ArH), 7.86 (s, 1H, C=CH), 7.92 (d, J = 4.8 Hz, 2H, ArH), 8.00 (d, J = 3.9 Hz, 2H, ArH), 8.13 (s, 2H, ArH). ^{13}C NMR ($CDCl_3$, 75 MHz) δ: 22.18, 26.45, 28.87, 43.29, 50.13, 61.94, 69.08, 109.55, 110.58, 112.16, 112.27, 116.76, 117.76, 121.23, 123.52, 123.66, 126.44, 128.74, 129.30, 129.86, 130.36, 133.55, 139.47, 145.29, 147.06, 148.63, 151.01, 155.43, 166.72. MALDI-TOF MS: calcd. for $C_{80}H_{77}N_{15}O_{14}$: m/z $[M+Na]^+$ 1093.5; found: m/z 1093.3. $C_{53}H_{50}N_8O_7Br_2$ (EA) (%) found: C, 59.33; H, 4.76; N, 10.32. Calcd. C, 59.45; H, 4.71; N, 10.47.

(3) Synthesis of monomer **MG1**. The procedure was similar to the synthesis of **MG0**. Chromophore **G1-≡** (170.9 mg, 1.0 mmol), compound **S2** (90.0 mg, 2.0 mmol). The crude product was purified by column chromatography on silica gel using THF/chloroform (1/2) as eluent to afford red solid **MG1** (200 mg, 93%). IR (KBr), υ (cm^{-1}): 1723 (C=O), 1511, 1341 (–NO_2). ^{1}H NMR ($CDCl_3$, 300 MHz) δ (TMS): 0.94 (t, J = 7.2 Hz , 4H, –CH_2–), 1.26 (s, br, 4H, –CH_2–), 1.77 (s, br, 2H, –CH_2C–), 1.86 (s, br, 2H, –CH_2–), 2.22–2.30 (m, 4H, –CH_2–), 2.26 (t, J =6.9 Hz, 4H, –CCH_2–), 3.70 (s, br, 4H, –NCH_2–), 3.93 (t, 4H, –NCH_2–), 4.11 (t, J = 6.3 Hz, 8H, –NCH_2–), 4.22 (t, J = 6.3 Hz, 4H, –NCH_2–), 4.35 (s, br, 4H, –OCH_2–), 4.56 (t, J = 6.0 Hz, 4H, –$COOCH_2$–), 6.52 (d, J = 4.5 Hz, 2H, –ArH–), 6.94 (d, J = 4.5 Hz, 6H, –ArH–), 7.24 (m, 8H, –ArH–), 7.32 (s, 3H, C=CH), 7.49–7.63 (m, 10H, ArH), 7.74–7.98 (m, 15H, ArH), 7.99 (d, J = 4.2 Hz, 12H, ArH), 8.11 (s, 2H, ArH). ^{13}C NMR ($CDCl_3$, 75 MHz) δ: 22.04, 26.79, 28.61, 28.87, 30.30, 43.28, 47.49, 50.13, 51.45, 61.94, 68.74, 109.40, 110.62, 112.12, 116.74, 117.69, 121.28, 122.62, 123.49, 126.46, 128.77, 129.28, 129.86, 133.58, 139.43, 145.16, 147.08, 147.40, 148.49, 151.04, 155.32, 166.72. MALDI-TOF MS: calcd. for $C_{80}H_{77}N_{15}O_{14}$: m/z $[M+Na]^+$ 2175.6; found: m/z 2175.5. $C_{109}H_{104}N_{22}O_{17}Br_2$ (EA) (%) found: C, 60.06; H, 5.393; N, 13.77. Calcd. C, 60.78; H, 4.87, N, 14.32.

(4) Synthesis of **DHPG0**. A mixture of dendonized A_2-type monomer **MG0** (96.9 mg, 0.09 mmol), B_3-type monomer **S3** (37.5 mg, 0.06 mmol), potassium carbonate (10 equiv), THF (9 mL)/water (1 mL), and $Pd(PPh_3)_4$ (5 mol%) was carefully degassed and charged with argon. Then the reaction mixture was stirred at 60°C for 9 h. Before gelation, an excess of methanol was poured into the mixture, then it was filtered. The obtained solid was dissolved in THF, and the insoluble solid was filtered out. After removal of the solvent, the residue was further purified by several precipitations from THF into acetone, and the obtained solid was then washed with an excess of acetone and dried in a vacuum at 40°C to a constant weight. The resultant polymer was obtained as a red powder (74.1 mg, 85.0%). M_w = 5400, M_w/M_n = 1.48, (GPC, polystyrene calibration). M_w = 95800, M_w/M_n = 1.15, (LLS). IR (KBr), υ (cm^{-1}): 1724 (C=O), 1518, 1336 (–NO_2). ^{1}H NMR ($CDCl_3$, 300 MHz) δ (TMS): 1.0–1.4 (–CH_2–), 1.4–2.0 (–CH_2–), 2.0–2.4 (–CH_2–), 2.8–3.0 (–CH_2–), 3.6–3.9 (–NCH_2–), 4.1–4.3 (–NCH_2– and –OCH_2–), 4.3–4.6 (–$COOCH_2$–), 6.7–7.0 (ArH), 7.0–8.0(ArH and C=CH), 8.33 (ArH). ^{13}C NMR ($CDCl_3$, 150 MHz) δ : 22.23, 26.52, 26.90, 28.71, 29.07, 30.30, 50.00, 61.89, 69.05, 109.45, 112.10, 121.21, 124.84, 126.41, 128.69, 129.80, 132.36, 133.49, 140.28, 145.21, 147.03, 150.99, 166.60.

(5) Synthesis of **DHPG1**. The procedure was similar to the synthesis of **DHPG0**. **MG1** (103.4 mg, 0.048 mmol), **S3** (19.9 mg, 0.032 mmol), reaction time: 21 h. The resultant polymer was obtained as a red powder (90.0 mg, 90.0%). M_w = 2600, M_w/M_n = 1.67, (GPC, polystyrene calibration). M_w = 60200, M_w/M_n = 1.37, (LLS). R (KBr), υ (cm^{-1}): 1724 (C=O), 1518, 1336 (–NO_2). ^{1}H NMR ($CDCl_3$, 300 MHz) δ (TMS): 1.0–1.4 (–CH_2–), 1.4–2.4 (–CH_2–), 2.6–3.0 (–CH_2–), 3.4–4.6 (–NCH_2– and –OCH_2–), 6.3–8.2 (ArH and C=CH). ^{13}C NMR ($CDCl_3$, 150Hz) δ : 20.81, 24.59, 25.23, 27.41, 46.20, 48.85, 50.14, 60.71, 66.94, 67.64, 108.32, 110.92, 115.41, 116.41, 121.35, 125.17, 125.59, 126.93, 127.47, 127.75, 128.57, 130.97, 132.27, 143.96, 145.85, 146.13, 147.23, 149.84, 154.11, 165.42.

1.3 Preparation of polymer thin films

The DHPs were dissolved in THF (concentration ~4 wt%), and the solutions were filtered through syringe filters, and the films were spin-coated onto indium-tin-oxide (ITO)-coated glass substrates, which were cleaned by *N*, *N*-dimethyformamide, acetone, distilled water and THF sequentially in ultrasonic bath before use. Residual solvent was removed by heating the films in a vacuum oven at 40°C.

1.4 NLO measurement of poled films

The second-order optical nonlinearity of the dendrimers was determined by *in-situ* second harmonic generation (SHG) experiment using a closed temperaturecontrolled oven with optical windows and three needle electrodes. The films were kept at 45° to the incident beam and poled inside the oven, and the SHG intensity was monitored simultaneously. Poling conditions were as follows: temperature: different for each polymer; voltage: 7.5 kV at the needle point; gap distance: 0.8 cm. The SHG measurements were carried out with a Nd: YAG laser operating at a 10 Hz repetition rate and an 8 ns pulse width at 1064 nm. A Y-cut quartz crystal served as the reference.

2 Results and discussion

2.1 Synthesis

Usually, the synthesis of dendronized polymers can be achieved by a graft-to, graft-from or macromonomer approach [20]. Similar to that, there should be also three approaches to synthesize DHPs. However, different from normal linear polymers, hyperbranched polymers were highly branched, and the reaction sites inside could be "protected" by the polymeric backbone. If graft-to or graft-from approach was used, the inevitable large steric effect could hinder the reaction seriously. Therefore, the macromonomer approach seemed to be the unique route. As shown in Figure 2, the B_2 type macromonomers, dibromo dendrionized carbazole **MG0** and **MG1**, were prepared *via* powerful Sharpless "click chemistry" reaction between **S2** and different generation dendrons **G0-≡** and **G1-≡** (the synthetic route was shown in Scheme S1 in supporting information). And, for the preparation of the target DHPs, the one-pot Suzuki polycondensation reaction was utilized between dibromo dendrionized carbazoles and B_3 type monomer **S3** (Figure 3). It was known that the "A_2+B_3" type

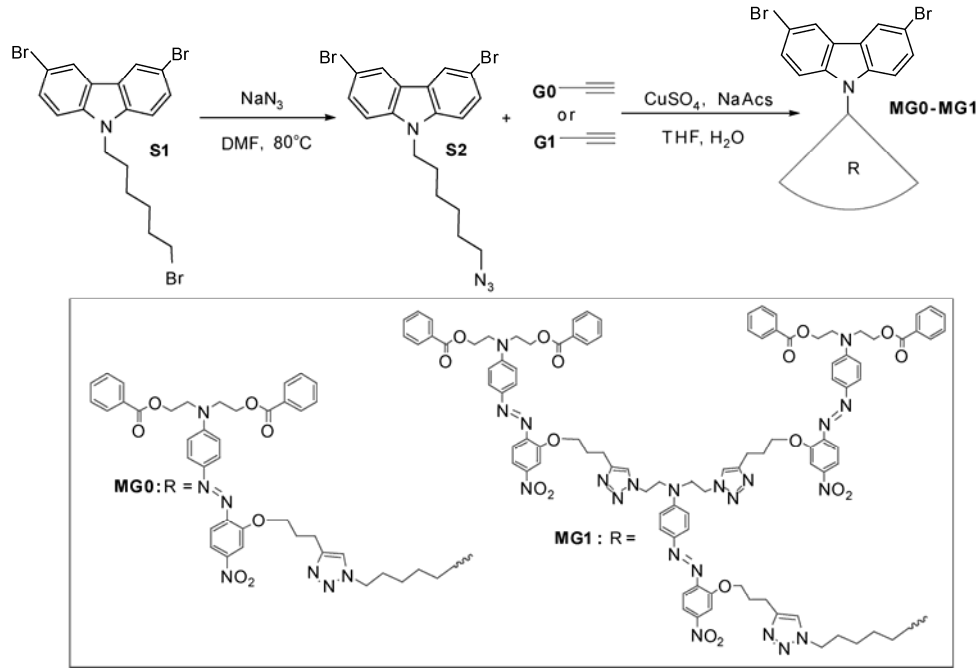

Figure 2 The synthesis of the monomers **MG0** and **MG1**.

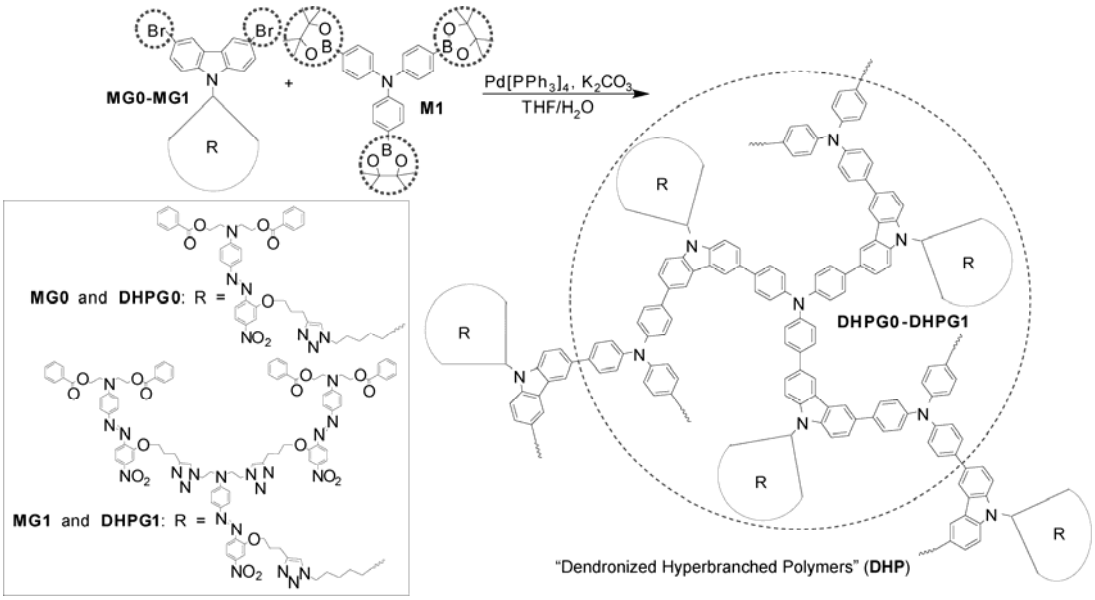

Figure 3 The synthesis of "dendronized hyperbranched polymers" **DHPG0** and **DHPG1**.

polymerization would lead to the formation of cross-linking insoluble polymer, the polymeric procedure thus must be controlled carefully. Here, an advantage could be noted once the dendronized monomer was used: the dendronized architecture had larger bulk than normal monomers, which could bring out the steric hindrance, and decrease the reactivity in the polymerization process, indicating that the polymerization could be more controllable, making the preparation of the soluble DHPs easy. However, if the steric effect was too large, the low reactivity also made the polymerization failed. This point could be also reflected in their different polymeric reaction time. For **DHPG0**, if the reaction time was longer than 9.5 h, the resultant hyperbranched polymers could not be dissolved in any solvent, while 22 h for **DHPG1**. Thus, in the reaction, the real times were a little shorter than the above ones (Table 1). In fact, the higher generation dendron containing DHP, **DHPG2**, was also attempted to be synthesized, but failed (Figure 4). After 48 h, there were still lots of reactants (**MG2** and **S3**) existed in the mixture, as tested by the thin layer chromatogram (TLC). This indicated that the too large steric hindrance of the dendrons hampered the polymerization. Also, the normal hyperbranched polymer with no dendrons in it was investigated to further confirm that the procedure for the preparation of these DHPs was more controllable (Figure 4). Under the same conditions, only 40 min later, the reaction solution became a little opaque, and only 1 h later, there was no soluble polymers obtained.

2.2 Characterizations

All of polymers and intermediates were characterized by spectroscopic methods (see Supporting Information for details: Figure S1 was their FT-IR spectra, Figures S2–S11 were their NMR spectra, Figures S12 and S13 were their MALDI-TOF mass spectra). Figure 5 showed the ^{1}H NMR spectra of **DHPG1** and its corresponding monomers as examples. In comparison with the ^{1}H NMR spectra of **S2** and **G1-≡**, some peaks disappeared, which could be assigned to the protons of the –CH_2N$_3$– in **S2** and –C≡C*H* (2.05) in **G1-≡**, while another peak, assigned to the proton of the new formed triazole, appeared. After polymerization, all the peaks showed an inclination of signal broadening obviously, indicating the polymerizations were successful. However, it was a pity that the degree of branching (DB) could not be calculated from the ^{1}H NMR spectra, due to the too broad and overlap peaks.

The M_w and PDI values of **DHPG0** and **DHPG1** were estimated by the laser light scattering (LLS) technique to be 95800, 1.15 and 60200, 1.37, respectively (Table 1), also

Table 1 Reaction time and molecular weights of these DHPs

No.	Yield (%)	t (h)[a]	M_w (g mol^{-1})[b]	M_w/M_n[b]	M_w (g mol^{-1})[c]	M_w/M_n[c]
DHPG0	85.0	9	5400	1.48	95800	1.15
DHPG1	90.0	21	2600	1.67	60200	1.37

a) The reaction times to avoid formation of gelation. b) Relative value estimated by GPC in THF on the basis of a polystyrene calibration. c) Absolute value measured in THF by the LLS technique.

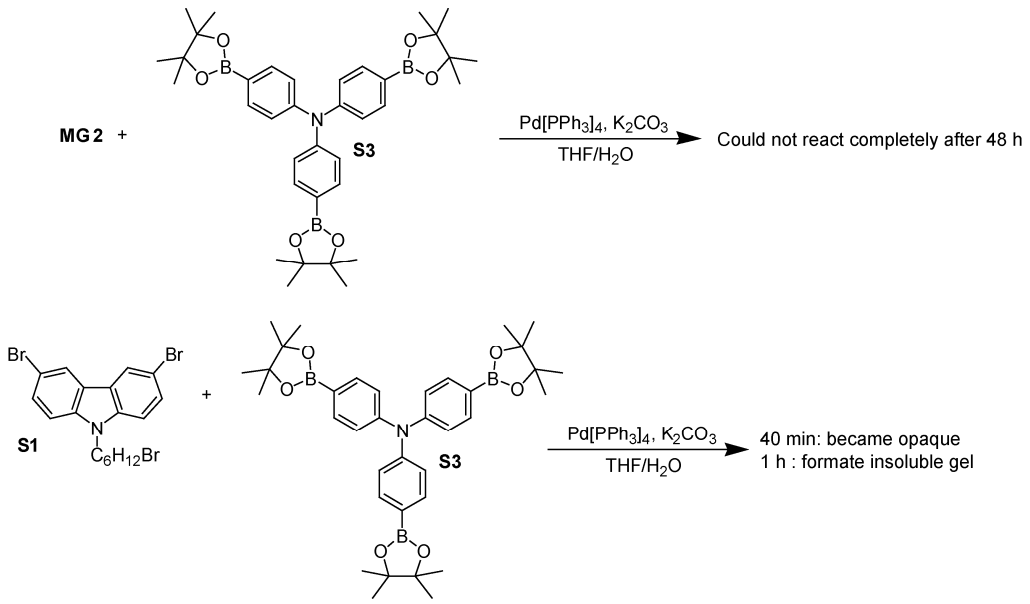

Figure 4 The different phenomena observed in the synthetic procedure of two model polymers.

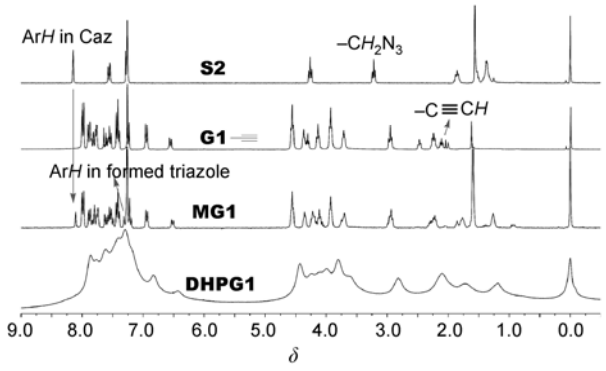

Figure 5 The ^{1}H NMR spectra of **DHPG1** and its corresponding monomers in chloroform-*d*.

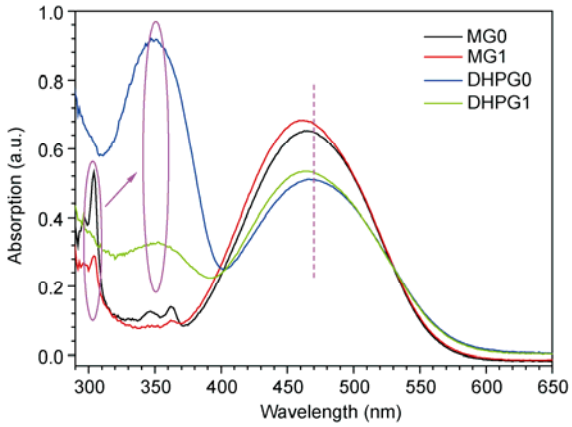

Figure 6 UV-vis spectra of THF solutions of **MG0**, **MG1, DHPG0** and **DHPG1** (0.02 mg/mL).

confirming the unique role during the polymerization of dendrons in these DHPs: their PDIs were all much lower than normal hyperbranched polymers, due to the more controllable polymerization procedure. Meanwhile, their relative molecule weights were also tested by gel permeation chromatography (GPC) on the basis of a polystyrene calibration (Table 1). Similar to normal dendritic macromolecules [21,22], their tested values were much smaller than their true ones, possibly due to the different hydrodynamic radius. This indicated that the obtained polymers were also highly branched as expected, although their DB values could not be calculated. Furthermore, the viscosity of these polymers was so low that could not be tested by an Ubbelohde viscometer, indicating their highly branched structure again.

The increase of conjugated system could make the absorption red-shifted. Here, after polymerization, the conjugated system of hyperbranched backbone could be enhanced in a large degree, which should be thus reflected in their UV-Vis spectra. As shown in Figure 3, there was an absorption peak at about 310 nm, which was the typical absorption of carbazole, in the monomers of **MG0** and **MG1**, this peak was shifted to 360 nm in **DHPG0** and **DHPG1**. This was another point to confirm the success of polymerization. Meanwhile, the maximum absorption wavelengths for the π–π* transition of the azo moieties in **DHPG1** was obviously blue-shifted than that in **DHPG0** (Figures 6, S14–S18 and Table S1), indicating that the dendronized structure could exhibit good site-isolation effect, directly reducing the strong intermolecular dipole-dipole interactions among chromophore moieties, and benefiting to the ordered noncentrosymmetric alignment of the chromophore moieties during the poling process in a large degree. In addition, the blue-shifted maximum absorption of **DHPG1** would surely result in their wide optical transparency window, and contribute to the practical application in photonics fields. These also reflected the usefulness of the dendrons in the side chain of hyperbranched polymers. However, as shown in Table S1, in comparison with dendrimers and dendronized polymers, these DHPs showed a little red-shift, which should be ascribed to their special topological structure. To know more information about this new topological structure, further researches were still needed.

These DHPs were thermally stable (Figure S19), with the 5% weight loss temperatures of 291 and 285°C, respectively. The glass transition temperature (T_g) of the DHPs were tested to be 140 and 138°C, respectively, by using differential scanning calorimetry (DSC). These results were encouraging. In our previous work on dendrimers **G1-G3** [16] (Scheme S1, Table S2) and dendronized polymers **PG0-PG2** [17] (Scheme S3, Table S2), the T_g values increased accompanying with the increasing of generation number, however, not higher than 96°C. Here, the T_g values were much higher, possibly due to their special topological structure, as well as their larger molecular weights. Furthermore, the higher T_g values could lead to higher stability of the ordered dipole alignment of NLO chromophores, and surely benefit to their potential practical applications.

2.3 NLO properties

The obtained **DHPG0** and **DHPG1** were soluble in common polar organic solvents, such as chloroform, THF, DMF and DMSO, and exhibited good film-forming ability. To evaluate the NLO activities, their poled films were prepared. The convenient technique to study the second-order NLO activity was to investigate the second harmonic generation (SHG) processes characterized by d_{33}, an SHG coefficient. The method for the calculation of the SHG coefficients (d_{33}) for the poled films has been reported in our previous papers [15–19]. From the experimental data, the d_{33} values of **DHPG0** and **DHPG1** were calculated to be 91 and 133 pm/V, respectively, at 1064 nm fundamental wavelength (Table 2). To check the reproducibility, we repeated the measurements three times and got the same results. In our previous work on the concept of "suitable isolation group", we have synthesized many NLO polymers [15]. Figure 7

Table 2 NLO results of DHPs

No.	T_e (°C)[a)]	l_s (μm)[b)]	d_{33} (pm V^{-1})[c)]	$d_{33(\infty)}$ (pm V^{-1})[d)]	Φ[e)]	N[f)]
DHPG0	145	0.22	91	13	0.12	0.278
DHPG1	140	0.22	133	21	0.18	0.415

a) The best poling temperature. b) Film thickness. c) Second harmonic generation (SHG) coefficient. d) The nonresonant d_{33} values calculated by using the approximate two-level model. e) Order parameter $\Phi = 1-A_1/A_0$, A_1 and A_0 are the absorbance of the polymer film after and before corona poling, respectively. f) The loading density of the effective chromophore moieties.

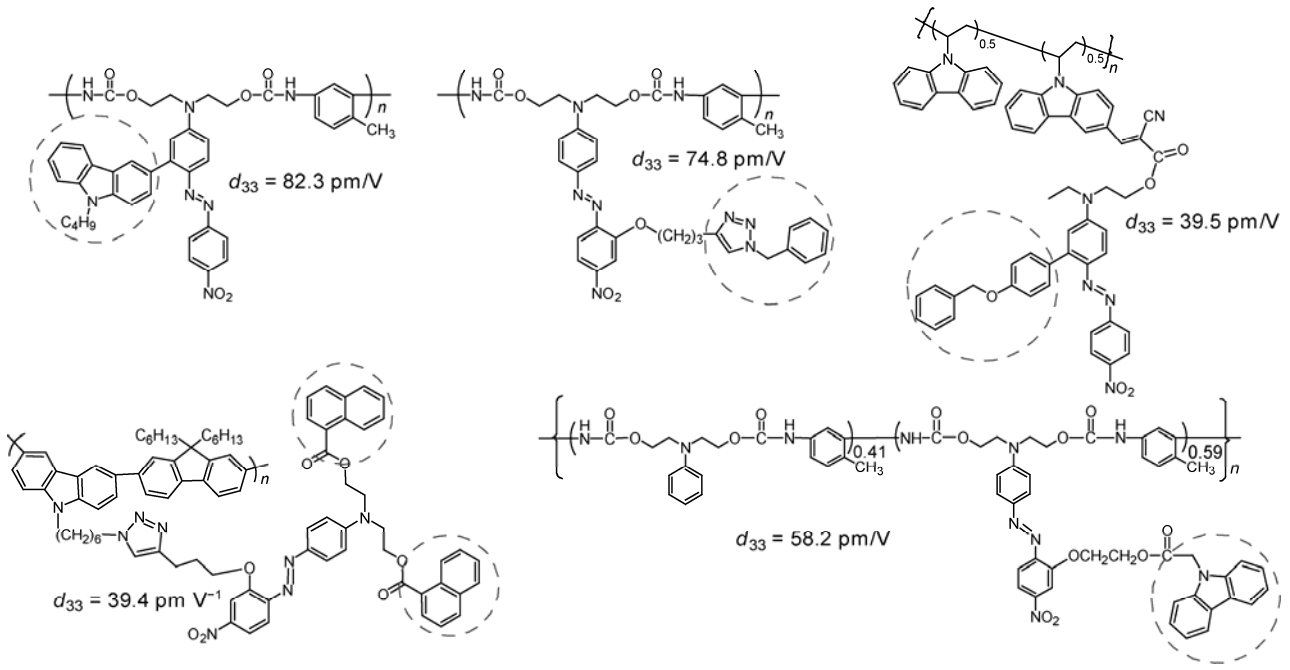

Figure 7 Some nitro azobenzene chromophore based NLO polymers and their d_{33} values.

showed some examples of nitro azobenzene chromophore based NLO polymers with suitable isolation group. It was obvious that the d_{33} values of these DHPs were relative high.

In our previous work on dendrimers **G1-G3** and dendronized polymers **PG0-PG2** (Table S2) [16,17], the d_{33} values increased, accompanying with the increasing loading density of the chromophore moieties, due to more and more perfect 3D structures. Here, the similar phenomenon appeared in these highly branched DHPs: accompanying with the loading concentration of the chromophore moieties changing from 0.278 in **DHPG0** to 0.415 in **DHPG1**, the measured NLO coefficient values increased from 91 (**DHPG0**) to 133 pm V^{-1} (**DHPG1**), as the 3D topological structure became better from **DHPG0** to **DHPG1**. Also, the isolation effect of the exterior phenyl moieties and the interior triazole rings could contribute much to its NLO coefficent, according to the concept of "suitable isolation group". Meanwhile, 133 pm V^{-1} was even higher than those of dendrimes (122.7 pm V^{-1} of **G3**) and dendronized polymers (106.0 pm V^{-1} of **PG2**), indicating that the hyperbranched backbone could also contribute much to their NLO coefficient. This point was very similar to normal hyperbranched polymers. In recent years, there were many literatures reporting that the NLO coefficient of hyperbranched polymers were higher than their linear analogues, due to site-isolation effect [23–25]. However, the DHPs were not the same to hyperbranched polymers, further researches were still needed to confirm the advantages of DHPs.

As the films of the DHPs still had some absorptions at the wavelength of 532 nm (the doubled frequency of the 1064 nm fundamental wavelength), the NLO properties of dendrimers should be smaller, as shown in Table 2 ($d_{33}(\infty)$), due to the resonant enhancement effect [26]. Because of their high d_{33} values and wide optical transparency window, the $d_{33}(\infty)$ value of **DHPG1** was still as high as 21 pm V^{-1}, higher than those of dendrimers (18.2 pm V^{-1} of **G3**) and dendronized polymers (19.9 pm V^{-1} of **PG2**), making these DHPs suitable for potential applications in optical fields.

To further explore the alignment of the chromophore moieties in these DHPs, we measured their order parameter (Φ) (Table 2 and Figures S20 and S21). According to the equation (footnote g in Table 2), the Φ values of DHPs were calculated and the results were listed in Table 2. The trend of the Φ values was the same as the d_{33} values of

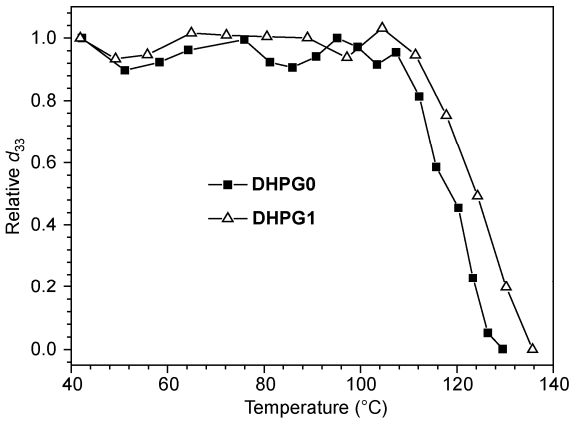

Figure 8 Decay curves of the SHG coefficients of DHPs as a function of the temperature.

DHPs.

Depoling experiments of DHPs were conducted, in which the real time decays of their SHG signals were monitored as the poled films were heated from 35 to 140°C in air at a rate of 4°C min^{-1}. Figure 8 displayed the decay of the SHG coefficient of these DHPs as a function of temperature. Due to their much higher T_g values, the temporal stability of dipole orientation of these dendrimers were also improved in a large degree: the temperatures for decay of dendrimers and dendronized polymers were only around 70°C (**G3** and **PG2**) [16,17], while the values of **DHPG0** and **DHPG1** were both higher than 105°C. This should be an important advantage of DHPs in the NLO field, in comparison with other types of dendritic macromelacues.

Suzuki polycondensation reaction, two dendronized hyperbranched polymers, **DHPG0** and **DHPG**, were prepared successfully and used as NLO materials. The obtained polymers displayed excellent solubility and processability. Furthermore, thanks to the special topological structure, **DHPG1** exhibited better NLO property (with the d_{33} value of 133 pm V^{-1}) and higher stability than its analogue of dendronized polymer and dendrimer. Further study on this special dendronized hyperbranched structure is still in progress in our laboratory.

This work was supported by the National Natural Science Foundation of China (*21034006*).

1 Walter M V, Malkoch M. Simplifying the synthesis of dendrimers: Accelerated approaches. Chem Soc Rev, 2012, 41: 4593–4609
2 Astruc D, Boisselier E, Ornelas C. Dendrimers designed for functions: From physical, photophysical, and supramolecular properties to applications in sensing, catalysis, molecular electronics, photonics, and nanomedicine. Chem Rev, 2010, 110: 1857–1959
3 Mintzer M A, Grinstaff M W. Biomedical applications of dendrimers: A tutorial. Chem Soc Rev, 2011, 40: 173–190
4 Scholl M, Kadlecova Z, Klok H A. Dendritic and hyperbranched polyamides. Prog Polym Sci, 2009, 34: 24–61
5 Tomalia D A. Birth of a new macromolecular architecture: Dendrimers as quantized building blocks for nanoscale synthetic polymer chemistry. Prog Polym Sci, 2005, 30: 294–324
6 Li Q, Zhong A, Liu H, et al. Two-photon absorption in V-type chromophores with electron-rich heterocyclevinylene bridges. Sci China Chem, 2011, 54: 625–630
7 Zhang J, Yang Y, He C, et al. Red-emission organic light-emitting diodes based on solution-processable molecules with triphenylamine core and benzothiadiazole-thiophene arms. Sci China Chem, 2011, 54: 695–698
8 Tomalia D A, Kirchhoff P M. Rod-shaped dendrimers. US Patent 4,694,064, 1987
9 Tomalia D A, Naylor A M, Goddard W A III. Starburst dendrimers: Molecular-level control of size, shape, surface chemistry, topology, and flexibility from atoms to macroscopic matter. Angew Chem Int Ed, 1990, 29: 138–175
10 Grayson S M, Fréchet J M J. Convergent Dendrons and dendrimers: From synthesis to applications. Chem Rev, 2001, 101: 3819–3867
11 Dalton L R, Sullivan P A, Bale D H. Electric field poled organic electro-optic materials: State of the art and future prospects. Chem Rev, 2010, 110: 25–55
12 Robinson B H, Dalton L R. Monte carlo statistical mechanical simulations of the competition of intermolecular electrostatic and poling-field interactions in defining macroscopic electro-optic activity for organic chromophore/polymer materials. J Phys Chem A, 2000, 104: 4785–4795
13 Robinson B H, Dalton L R, Harper H W, et al. The molecular and supramolecular engineering of polymeric electro-optic materials. Chem Phys, 1999, 245: 35–50
14 Kanis D R, Ratern M A, Marks T J. Design and construction of molecular assemblies with large second-order optical nonlinearities. Quantum chemical aspects. Chem Rev 1994, 94: 195–242
15 Li Z, Li Q, Qin J. Some new design strategies for second-order nonlinear optical polymers and dendrimers. Polym Chem, 2011, 2: 2723–2740
16 Li Z, Yu G, Wu W, et al. Nonlinear optical dendrimers from click chemistry: Convenient synthesis, new function of the formed triazole rings, and enhanced NLO effects. Macromolecules, 2009, 42: 3864–3868
17 Li Z, Yu G, Liu Y, et al. Dendronized polyfluorenes with high azo-chromophore loading density: Convenient synthesis and enhanced second-order nonlinear optical effects. Macromolecules, 2009, 42: 6463–6472
18 Li Z, Wu W, Li Q, et al. High-generation second-order nonlinear optical (NLO) dendrimers: Convenient synthesis by click chemistry and the increasing trend of NLO effects. Angew Chem Int Ed, 2010, 49: 2763–2767
19 Wu W, Huang L, Song C, et al. Novel global-like second-order nonlinear optical dendrimers: Convenient synthesis through powerful click chemistry and large NLO effects achieved by using simple azo chromophore. Chem Sci, 2012, 3: 1256–1261
20 Frauenrath H. Dendronized polymers—building a new bridge from molecules to nanoscopic objects. Prog Polym Sci, 2005, 30: 325–384
21 Muchtar Z, Schappacher M, Deffieux A. Hyperbranched nanomolecules: Regular polystyrene dendrigrafts. Macromolecules, 2001, 34: 7595–7600
22 Kim Y, Webster O W. Hyperbranched polyphenylenes. Macromolecules, 1992, 25: 5561–5572
23 Li Z, Wu W, Ye C, et al. New hyperbranched polyaryleneethynylene containing azo-benzene chromophores in the main chain: Facile synthesis, large optical nonlinearity and high thermal stability. Polym Chem, 2010, 1: 78–81
24 Li Z, Wu W, Ye C, et al. New second-order nonlinear optical polymers derived from AB_2 and AB monomers via Sonogashira coupling reaction. Macromol Chem Phys, 2010, 211: 916–923
25 Wu W, Ye C, Qin J, et al. A series of AB_2-type second-order nonlinear optical (NLO) polyaryleneethynylenes: Using different end-capped spacers with adjustable bulk to achieve high NLO coefficients.

Polym Chem, 2013, 4: 2361–2370
26 Kauranen M, Verbiest T, Boutton C, et al. Supramolecular second-order nonlinearity of polymers with orientationally correlated chromophores. Science, 1995, 270: 966–969

Supporting Information

Scheme S1 The synthetic route to the dendrons (**G0-≡**, **G1-≡** and **G2-≡**).
Scheme S2 The synthetic route to B_3 type monomer **S3**.
Figure S1 The FT-IR spectra of DHPs and their corresponding monomers.
Figure S2 ^{1}H NMR spectrum of **S2** in chloroform-*d*.
Figure S3 ^{13}C NMR spectrum of **S2** in chloroform-*d*.
Figure S4 ^{1}H NMR spectrum of **MG0** in chloroform-*d*.
Figure S5 ^{13}C NMR spectrum of **MG0** in chloroform-*d*.
Figure S6 ^{1}H NMR spectrum of **MG1** in chloroform-*d*.
Figure S7 ^{13}C NMR spectrum of **MG1** in chloroform-*d*.
Figure S8 ^{1}H NMR spectrum of **DHPG0** in chloroform-*d*.
Figure S9 ^{13}C NMR spectrum of **DHPG0** in chloroform-*d*.
Figure S10 ^{1}H NMR spectrum of **DHPG1** in chloroform-*d*.
Figure S11 ^{13}C NMR spectrum of **DHPG1** in chloroform-*d*.
Figure S12 The MALDI-TOF mass spectrum of **MG0**.
Figure S13 The MALDI-TOF mass spectrum of **MG1**.
Figure S14 UV-Vis spectra of 1,4-dioxane solutions of **DHPG0** and **DHPG1** (0.02 mg/mL).
Figure S15 UV-Vis spectra of chloroform solutions of **DHPG0** and **DHPG1** (0.02 mg/mL).
Figure S16 UV-Vis spectra of dichloromethane solutions of **DHPG0** and **DHPG1** (0.02 mg/mL).
Figure S17 UV-Vis spectra of DMF solutions of **DHPG0** and **DHPG1** (0.02 mg/mL).
Figure S18 UV-Vis spectra of DMSO solutions of **DHPG0** and **DHPG1** (0.02 mg/mL).
Table S1 The maximum absorption of DHPs (λ_{max} (nm), 0.02 mg/mL)
Figure S19 TGA thermograms of **DHPG0** and **DHPG1**, measured in nitrogen at a heating rate of 10°C/min.
Scheme S3 The synthetic route to the dendronized polymers **PG0-PG2**.
Table S2 Physical and NLO results of dendrimers and dendronized polymers
Figure S20 Absorption spectra of the film of **DHPG0** before and after poling.
Figure S21 Absorption spectra of the film of **DHPG1** before and after poling.

The supporting information is available online at csb.scichina.com and www.springerlink.com. The supporting materials are published as submitted, without typesetting or editing. The responsibility for scientific accuracy and content remains entirely with the authors.